Evaluation of a Decoupling-Based Fault Detection and Diagnostic Technique – Part I: Field Emulation Evaluation

Haorong Li
Ph.D, Assistant Professor
University of Nebraska-Lincoln
Omaha, Nebraska, USA
haorongli@unlnotes.unl.edu

James E. Braun
Ph.D., P.E .Professor
Purdue University
West Lafayette, Indiana, USA
jbraun@purdue.edu

Abstract: Existing methods addressing automated fault detection and diagnosis (FDD) for vapor compression air conditioning system have good performance for faults that occur individually, but they have difficulty in handling multiple-simultaneous faults. The decoupling-based (DB) FDD method explicitly addresses diagnostics for multiple-simultaneous faults for the first time. This paper is the first part of a two-part evaluation of the DB FDD technique whose intent is to validate the DB FDD performance and demonstrate its applications. The first part focuses on sensitivity and robustness evaluation through controlled field emulation testing. Sensitivity tests with artificially introduced faults show that individual faults can be identified before they cause a 5% of degradation in cooling capacity, EER and sensible heat ratio. Robustness tests for forty-one multiple-simultaneous-fault combinations demonstrate that no wrong diagnosis occurs with only two false alarms and two sensitivity losses for a liquid-line restriction. The second part, accompanying the first one, focuses on field applications in California [1].

Key words: fault detection and diagnostics; air conditioning; decoupling; multiple faults

1. INTRODUCTION

Fault detection and diagnosis (FDD) aims at early identification and isolation of premature faults that are not severe enough to cause significant performance degradation or equipment failure so that corrective measures can be taken proactively. A growing number of publications related to FDD have appeared in the last decade [2, 3]. According to the IEA ANNEX 34 final report edited by Dexter and Pakanen [4], twenty-three prototype FDD performance monitoring tools and three validation tools have been developed, thirty demonstrations have been taken place in twenty buildings, twenty-six FDD tools have been tested in real buildings, and four performance monitoring schemes have been jointly evaluated on three documented data sets from real buildings. Since 2001, 39 more papers have appeared [3] (Li, 2004). Katipamula and Brambley [5, 6] conducted a thorough review on methods for automated FDD and prognostics for building systems. This review provided a framework for categorizing methods, identified their primary strengths and weaknesses, addressed their applications specific to the fields of HVAC&R, and briefly discussed the future of automated diagnostics in buildings. In sum, existing methods addressing automated FDD for vapor compression air conditioning equipment have good performance for faults that occur individually, but have difficulty in handling multiple-simultaneous faults. In addition, these methods either require high cost measurements or measurements over a wide range of conditions for training reference models, the development of which can be time consuming and cost-prohibitive.

Li and Braun [7] developed a fault detection and diagnosis method that can handle multiple faults using features that decouple the impacts of individual faults. The decoupled features are determined using virtual sensors that incorporate models and low-cost measurements. The models are simple and obtainable from information and data readily available from equipment manufacturers and do not require extensive training.

Fig. 1 depicts different models and their inputs and outputs for the FDD method of Li and Braun [7]. The inputs include both actual measurements (circled symbols) and variables determined from virtual sensors or simple combinations of actual measurements (bare symbols). The outputs are decoupled features (symbols within shaded ovals) and virtual sensor outputs needed by other modules. Many of the features and virtual sensors rely on quasi-steady performance. Quasi-steady state is a condition where the state variables are close to their equilibrium values for a given set of external driving conditions. A steady-state detector is required for implementation of this FDD method.

The FDD method considers important and difficult to diagnose faults that impact system cooling capacity, efficiency and equipment life as documented by Breuker and Braun [8], including faults that degrade compressor flow capacity (e.g., compressor valve leakage), low or high refrigerant charge (leakage or inadequate charging during service), air-side fouling or loss of flow for the condenser or evaporator, a liquid-line restriction (e.g., filter/dryer clogging), and presence of a non-condensable gas.

For the evaluations in this paper, the FDD method was applied in a post processing mode after data were collected. The combination of slope and variance methods [9] was used to determine quasi-steady conditions for the data sets that were obtained. In addition to the measurements shown in Fig. 1 (circled symbols), compressor power was measured for the purpose of evaluating fault impact. Cooling capacity was calculated from measured states and a virtual sensor for refrigerant flow [10]. Only the steady-state method for liquid-line restriction faults was employed as described by Li and Braun [10]. Improved FDD performance for this fault would undoubtedly be achieved using the transient method of Li and Braun [10]. However, this method was not available at the time testing was performed and therefore no transient data is available. In addition, non-condensable gas faults were not considered.

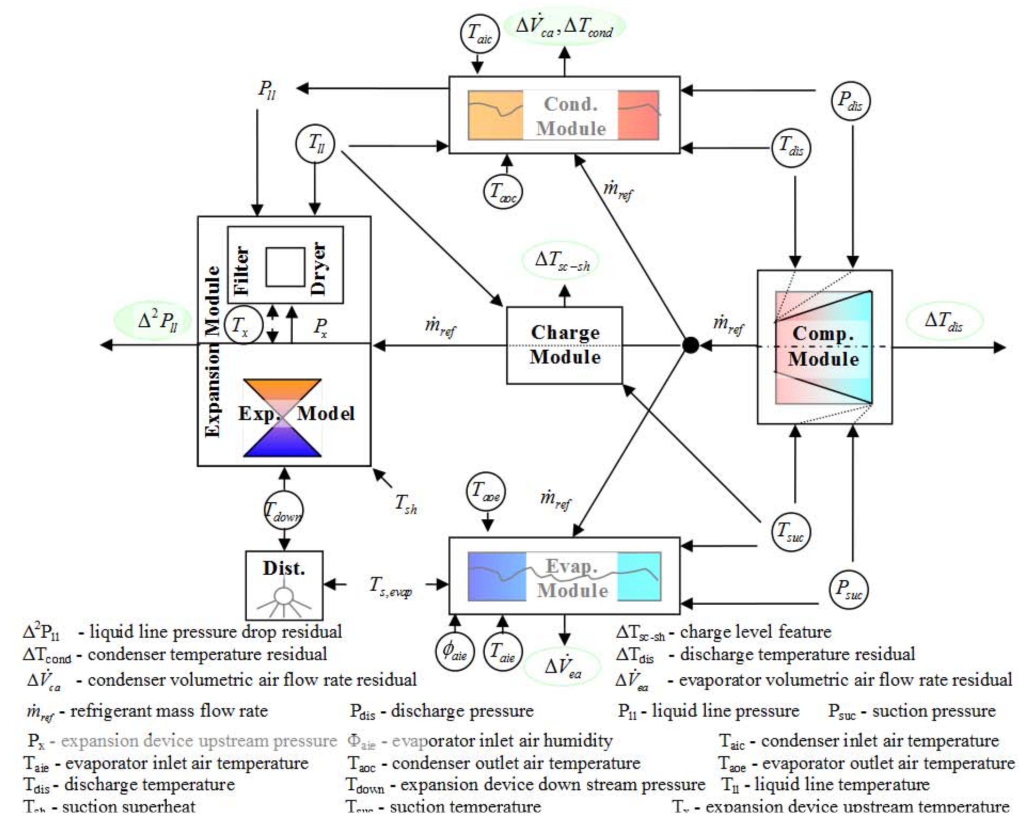

Fig. 1 FDD modules and their inputs and outputs

A simple diagnostic classifier was employed with a normalized fault indicator defined as

$$IND_{faultname} = \frac{fv_{current}}{fv_{range}}$$

where $IND_{faultname}$ denotes the decoupling fault feature for a given fault ($faultname$), $fv_{current}$ denotes the current feature value, and fv_{range} is a predefined range of interest for the feature value. For results presented in this paper, fv_{range} was chosen as the feature value at an individual fault level causing approximately a 20% cooling capacity degradation. FDD thresholds for the normalized indicators were at 0.2 (i.e., approximately 4% capacity degradation). The method can generally diagnose faults at lower levels, but at lower levels the fault impact is thought to be insignificant. Tab. 1 summarizes values for fv_{range} that were employed in this study.

Tab. 1 Predefined feature values and thresholds.

Fault name	Feature	fv_{range}	Threshold
compleak	ΔT_{dis}	15 (F)	0.2
condfoul	$\Delta \dot{V}_{ca}$	$0.25\dot{V}_{ca,setting}$	0.2
evapfoul	$\Delta \dot{V}_{ea}$	$0.25\dot{V}_{ea,setting}$	0.2
llrestr	$\Delta^2 P_{ll}$	4.4 (bar)	0.2
reflow	ΔT_{sc-sh}	10 (F)	0.2
refhigh	ΔT_{sc-sh}	10 (F)	-0.2

2. TESTING FACILITY

A 5-ton rooftop air condition was installed at Purdue University to mimic field-setups in California in order to aid in the identification of installation and operational problems locall and allow testing of alternative sensors and artificial introducing of faults, both of which would be logistically difficult to perform in California. The Purdue field test site is located at the storage room of the technical shop of Ray W. Herrick Laboratories. The 5-ton unit has a SEER of about 11. This unit uses a TXV as the expansion device and a constant, hermetically sealed scroll compressor. The evaporator blower uses a direct-drive motor with three speed options (nominal flow rate is 2000 cfm for middle speed option), while the condenser fan is single-speed with a nominal flow rate of 4500 cfm. The standard system charge is 9 lbs and 8 oz R22. . The measurements used for FDD tests are:

- Temperature measurements: evaporating temperature, suction line temperature, discharge line temperature, condensing temperature, liquid line temperatures before and after filter/drier temperature, expansion device down stream temperature, air temperatures of the condenser inlet and outlet, and dry bulb temperature and relative humidity of the the mixed air.
- Refrigerant pressure measurements: suction line pressure and discharge line pressure for the compressor.
- Power transducer to measure power consumption of the compressor.

Tab. 2 tabulates the method of implementing faults and corresponding fault levels simulated. Six faults were implemented in the Purdue field site: compressor valve leakage (Compleak), condenser fouling (Condfoul), evaporator fouling (Evapfoul), liquid-line restriction (Llrestr), low refrigerant charge (Reflow), and refrigerant high charge (Refhigh). Except for refrigerant charge and compressor leakage faults for which five fault levels were introduced, four fault levels were introduced for the other three faults. Since tests were performed in a field setting, the driving conditions were uncontrollable. Typically, they were conducted in the afternoon (from around 1:30 pm to 8:00 pm) when there was no direct solar radiation striking the condenser or its air outlet sensors. Most of the tests were performed in the summer and fall of 2003 and some of them were conducted in the spring of 2004.

3. SENSITIVITY EVALUATION

The sensitivity of the FDD technique is defined as the lowest fault level introduced to the system that could be successfully detected and diagnosed (the diagnostic thresholds of Tab. 1 were not employed). Below these levels, the FDD method could not reliably diagnosis faults. Since there are infinite combinations of multiple faults with different fault levels, sensitivity was only evaluated for individual faults. Since the implementation of each fault at different levels of Tab. 2 took from three to four hours in a single afternoon driving conditions changed. However, there were no drastic changes in temperature and humidity. Therefore, although sensitivities in terms of physical level were stable, sensitivities in terms of performance degradation may have small variations, due to the effects of driving conditions.

Tab. 3 summarizes the FDD sensitivity results. The levels at which faults could be diagnosed are expressed in several different ways: 1) fault level (from Tab. 2), 2) physical level (from Tab. 2 definitions), 3) % degradation in unit cooling capacity, 4) % degradation in unit EER, and 5) % degradation in unit sensible heat ratio (SHR). Since the fault levels were introduced at discrete levels, the first level represents the best possible sensitivity for these tests. The method could detect low refrigerant charge and loss of compressor performance at the lowest levels introduced and all other faults at the second level. All of the faults could be reliably diagnosed before a 5% degradation in capacity, EER, or SHR.

False alarm is an indication of a fault when in actuality a fault has not occurred. For a given technique, there is an inherent tradeoff between minimizing the false alarms and maximizing sensitivity. Tab. 4 lists the theoretical false alarm rates calculated from the fault indicator standard deviation at the FDD thresholds. Except for the liquid-line restriction, all the other faults had very small false alarm rates. Since the sensitivity of liquid-line restriction is high, it seems that there is some potential to reduce its false alarm rate by means of raising the FDD threshold further. However, robustness tests show that it is impractical to raise the FDD threshold.

4 ROBUSTNESS EVALUATION

4.1 Robustness Against multiple-faults

To verify robustness, multiple-simultaneous faults combinations of six faults were considered. Only one fault level was implemented for each combination, because there are infinite combinations if fault level is considered. Tab. 5 describes the individual fault levels implemented for multiple-simultaneous fault tests.

Tab. 2 Method of implementing faults and corresponding fault levels simulated.

Faults	Fault Introduction Method	Fault Level Expression	Fault Level Simulated					
			0	1	2	3	4	5
Compleak	Partially open a bypass valve between discharge and suction	% refrigerant mass flow rate bypass	0%	8%	18%	33%	44%	56%
Condfoul	Partially block condenser air flow with paper	% reduction of air volume flow rate	0%	3%	10%	13%	16%	
Evapfoul	Partially block evaporator air flow with paper	% reduction of air volume flow rate	0%	5%	9%	16%	31%	
Llrestr	Partially close the needle valve on the liquid line	% of the pressure drop from high to low sides	0%	5%	10%	13%	19%	
Reflow	Under-charge the system	% reduction of charge	0%	11%	16%	21%	26%	32%
Refhigh	Over-charge the system	% increase of charge	0%	11%	16%	21%	26%	32%

Tab. 3 FDD sensitivity for individual faults.

Faults	Simulated Level	Physical Level	Capacity Degradation	EER Degradation	SHR Degradation
Compleak	1st	8%	5%	3%	-3%
Condfoul	2nd	10%	3%	4%	0%
Evapfoul	2nd	9%	5%	4%	4%
Llrestr	2nd	10%	3%	1%	2%
Reflow	1st	11%	3%	1%	5%
Refhigh	2nd	16%	2%	2%	0%

Tab. 4 Fault indicator standard deviations of normal operations and false alarm rates.

Fault Name	Compleak	Condfoul	Evapfoul	Llrestr	Reflow	Refhigh
FDD Threshold	0.2	0.2	0.2	0.2	0.2	-0.2
Standard Deviation	0.072	0.074	0.091	0.133	0.066	0.066
False Alarm Rate	0.003	0.004	0.014	0.067	0.005	0.005

Tab. 5 Individual fault levels implemented for multiple-simultaneous fault tests.

Test No.	compleak	condfoul	evapfoul	llrestr	reflow	refhigh	Capacity Deg.	EER Deg.	SHR Deg.
1	27%	0	0	0	14%	0	28%	19%	-6%
2	27%	11%	0	0	14%	0	31%	25%	-9%
3	25%	11%	12%	0	11%	0	25%	20%	-6%
4	25%	11%	12%	12%	11%	0	27%	22%	-4%
5	0	11%	12%	12%	11%	0	9%	12%	14%
6	0	0	12%	12%	11%	0	5%	4%	12%
7	0	0	0	12%	14%	0	5%	0%	10%
8	29%	0	0	12%	14%	0	30%	21%	-6%
9	25%	0	12%	12%	11%	0	26%	17%	-2%
10	25%	0	12%	0	11%	0	25%	17%	0%
11	0	0	12%	0	11%	0	4%	1%	10%
12	0	11%	12%	0	11%	0	5%	9%	8%
13	0	11%	0	0	14%	0	6%	7%	4%
14	0	11%	0	12%	14%	0	6%	6%	10%
15	29%	11%	0	12%	14%	0	29%	23%	-7%
16	32%	11%	0	0	0	0	34%	28%	-18%
17	21%	11%	12%	0	0	0	25%	21%	-2%
18	21%	11%	12%	12%	0	0	21%	17%	-3%
19	0	11%	12%	12%	0	0	6%	10%	9%
20	0	0	12%	12%	0	0	1%	0%	8%
21	19%	0	12%	12%	0	0	21%	14%	-2%
22	32%	0	0	12%	0	0	33%	24%	-15%
23	0	11%	0	12%	0	0	-3%	4%	2%
24	32%	11%	0	12%	0	0	28%	25%	-15%
25	0	11%	12%	0	0	0	6%	10%	6%
26	19%	0	12%	0	0	0	20%	13%	-5%
27	33%	0	0	0	0	21%	30%	23%	-16%
28	32%	11%	0	0	0	21%	28%	24%	-17%
29	35%	11%	16%	0	0	21%	39%	35%	-9%
30	35%	11%	16%	12%	0	21%	36%	33%	-9%
31	0	11%	16%	12%	0	21%	8%	15%	8%
32	0	0	16%	12%	0	21%	7%	8%	9%
33	0	0	0	12%	0	21%	-3%	-1%	0%
34	32%	0	0	12%	0	21%	32%	25%	-13%
35	35%	0	16%	12%	0	21%	38%	31%	-6%
36	35%	0	16%	0	0	21%	38%	31%	-7%
37	0	0	16%	0	0	21%	7%	8%	8%
38	0	11%	16%	0	0	21%	8%	15%	7%
39	0	11%	0	0	0	21%	3%	10%	-1%
40	0	11%	0	12%	0	21%	3%	11%	1%
41	32%	11%	0	12%	0	21%	34%	31%	-16%

Tab. 6 Faults indicators for the different faults.

Fault	Compnv	Condfoul	Evapfoul	Llrestr	Reflow	Refhigh
Indicator number	1	2	3	4	5	6

Except for compressor leakage, all the other faults were implemented at the levels between the first diagnosed and next levels. Compressor leakage was implemented at different and relatively high fault levels because 1) a compressor leakage fault is completely decoupled from the other faults and has the highest robustness while other faults are unilaterally decoupled from it, 2) various compressor leakage faults are required to test the fault evaluation algorithm, and 3) high levels of compressor leakage faults are better for robustness tests of other faults. Fault levels of condenser fouling and liquid-line restriction and refrigerant overcharge were fixed, while two fault levels of low refrigerant charge and evaporator fouling were simulated and compressor leakage fault levels ranged from 20% to 35%. Since refrigerant charge faults are mutually exclusive, the total number of combinations is the sum of those at low charge,

$$C_4^2 + C_4^3 + C_4^4 = 11,$$

and high charge,

$$C_r^1 + C_4^2 + C_4^3 + C_4^4 = 15 .$$

All forty-one combinations with individual fault levels implemented are listed in Tab. 5. All the possible forty-one combinations were considered. For reference, indicators for the different faults are given in Tab. 6. Fig. 2 shows the different combinations of faults implemented for the forty-one different cases and also shows differences between binary indicators (1=fault, 0=no fault) for individual diagnosed and implemented faults. A '−1' denotes a missed diagnosis or sensitivity loss for one fault and a '1' denotes a false alarm. There were two false alarms and two missed diagnoses (lost sensitivity) for combinations with a liquid-line restriction. As previously noted, only the steady-state method presented by Li and Braun [10] was employed for liquid-line restriction. It is expected that the false alarms and missed diagnoses would be eliminated using the transient method of Li and Braun [10].

4.2 Detailed Robustness Evaluation

In order to quantify the robustness, a normalized indicator error, ρ_i, is defined as

$$\rho_i = \frac{IND_{i,MSF} - IND_{i,SF}}{\left| IND_{i,SF} - \left| IND_{i,threshold} \right| \right|}$$

where i is the individual fault name, $IND_{i,SF}$ is the fault indictor of fault i occurring individually, $IND_{i,MSF}$ is the fault indicator of fault i occurring simultaneously with other faults, $IND_{i,threshold}$ is the FDD threshold of fault i. Tab. 7 summarizes meanings of ρ_i for different cases.

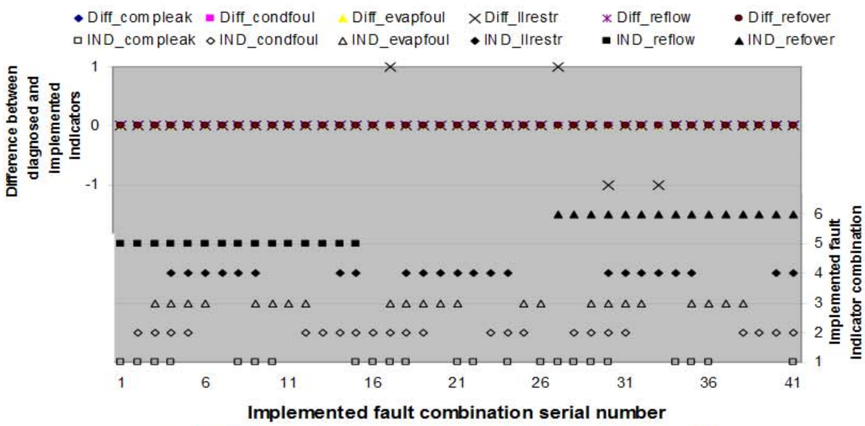

Fig. 2 Robustness tests for multiple-simultaneous-fault FDD

Tab. 7 Normalized fault indicator error and its meaning

Case	$\|\rho_i\| < 1$	When it is normal		When it is faulty	
		$\rho_i \le -1$	$\rho_i \ge 1$	$\rho_i \le -1$	$\rho_i \ge 1$
Refhigh		False alarm	False alarm	Sensitivity gain	Wrong Diagnosis
Reflow	OK	False alarm	False alarm	Wrong Diagnosis	Sensitivity gain
Other faults		OK	False alarm	Sensitivity loss	Sensitivity gain

Fig. 3 plots the normalized fault indicator error for compressor leakage. It can be seen that there were no false alarms and sensitivity losses or gains. The normalized fault indicator error is much smaller for faulty operation than for normal operation, meaning that the fault indicator has very good robustness against noise and uncertainties and high sensitivity to faults. For faulty operation, the noise and uncertainties are suppressed by high sensitivity, meaning that it is less likely to have sensitivity loss for faulty operation. This confirms the prior theoretical analysis: compressor valve leakage fault is completely decoupled from the other faults.

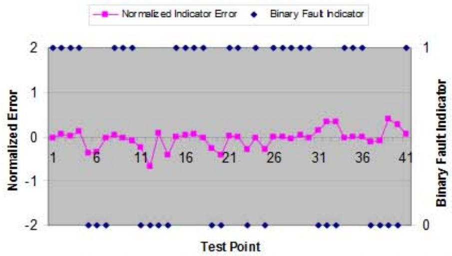

Fig. 3 FDD robustness for compressor leakage

The normalized fault indicator error for condenser fouling fault is given in Fig. 4. It can be seen that all the points are within the robustness boundaries and there is no obvious difference in robustness between normal operation and faulty operation. Although there were no false alarms and sensitivity losses, robustness was not as good as for compressor valve leakage. There are two factors which affect its robustness: 1) refrigerant mass flow rate estimation and 2) condenser outlet refrigerant enthalpy estimation. It seems that the compressor model and refrigerant mass flow rate correction algorithm have good performance. Theoretical analysis show that if the condenser outlet refrigerant quality is larger than 0.1, the relative error in enthalpy estimation is less than 5%. If the refrigerant charge is more than 50% of the nominal value, the condenser outlet refrigerant quality will not be less than 0.1.

In Fig. 5, the normalized fault indicator error for evaporator fouling is plotted. It can be seen that there is one point which is out of the range of the robustness boundaries and three points are marginally within the boundaries. However, the point outside the lower boundary does operate normally, so it will not cause any sensitivity loss. Overall, robustness for evaporator fouling was not as good as for compressor leakage and condenser fouling but there were no false alarms and sensitivity losses. There are three factors which affect its robustness: 1) refrigerant mass flow rate estimation, 2) condenser outlet refrigerant enthalpy estimation, and 3) evaporator outlet air enthalpy estimation. Since there is no humidity sensor for evaporator outlet air, its enthalpy is estimated using a virtual sensor, which adds some additional noise and uncertainty.

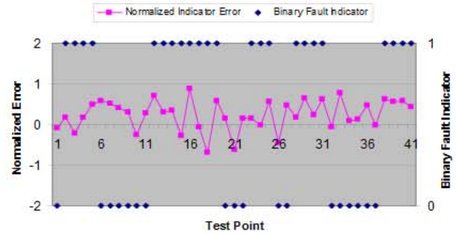

Fig. 4 FDD robustness for condenser fouling

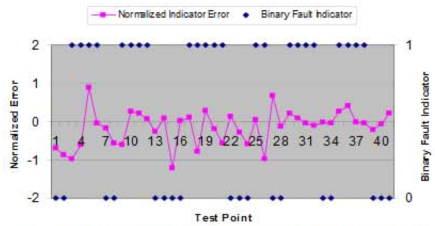

Fig. 5 FDD robustness for condenser fouling

The normalized liquid-line restriction fault indicator error is shown in Fig. 6. It can be seen that there are 6 points which are out of the robustness boundaries. Two of them operating normally are outside of the upper boundary and cause false alarms. Another two operating abnormally are outside of the lower boundary and cause sensitivity losses. The other two of them operating abnormally are outside the upper boundary and cause sensitivity gain. There are three points which are marginally within the boundary.

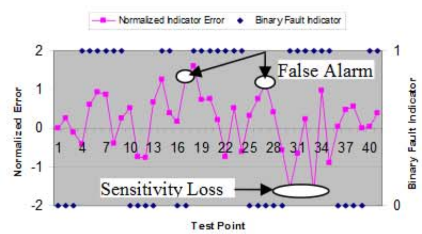

Fig. 6 FDD robustness for liquid-line restriction.

The reason for worse robustness is that more uncertainties are introduced: 1) refrigerant mass flow rate estimation, 2) condenser outlet refrigerant pressure estimation, and 3) estimation of pressure drop across the TXV. Pressure drop across the TXV is estimated using a TXV model which is pretty sensitive to superheat measurement noise and refrigerant mass flow rate estimation. In addition, when the operation is out of the control range of the TXV, the TXV model will not have good performance. There are two situations where this will occur: 1) when the refrigerant charge is lower than a certain value, the TXV is saturated and will cause abnormally high superheat, and 2) when there is a compressor leakage fault, the evaporating pressure may be high enough to trigger the TXV maximum operation pressure (MOP). In addition to more uncertainties, the pressure drop across the clogged filter/drier itself varies according to refrigerant mass flow rate and refrigerant state even for the same physical fault level. As previously noted, it is expected that the false alarms and missed diagnoses would be eliminated if the transient method of Li and Braun [10] were employed for liquid-line restriction faults.

The normalized fault indicator error for both refrigerant low and high charge is plotted in Fig. 7. For the refrigerant low charge fault, there are 3 points which are outside of the upper boundary which indicates sensitivity gain, and there were no wrong diagnoses and sensitivity losses. When the refrigerant is normally and over charged, all the test points are within the robustness boundaries and there are no false alarms and sensitivity losses.

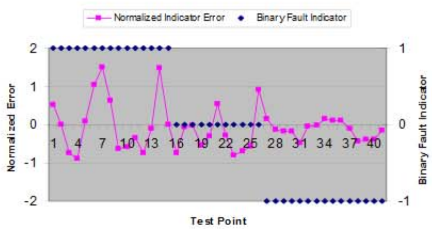

Fig. 7 FDD robustness testing for refrigerant charge faults.

The last three columns of Tab. 5 tabulate all fault impacts for the different tests in terms of performance degradations in capacity, EER, and SHR. Some combinations of faults cause very significant performance impacts and service would be justified. Generally, faults have a more significant effect on capacity than EER. The impact on SHR is even less. However, in some cases faults increase latent removal (reduced SHR) which leads to increased cooling loads and greater operating costs. On the other hand, an increased SHR could lead to comfort problems.

5 CONCLUSIONS

This paper presents a detailed evaluation of the FDD method of Li and Braun [7, 10]. Faults are artificially introduced into a rooftop air conditioner at different levels in order to evaluate sensitivity and robustness of the method. Sensitivity tests show that all the individual faults can be identified before they cause a 5% of degradation in cooling capacity, EER and SHR. Robustness tests of 41 multiple simultaneous fault combinations demonstrate that no wrong diagnosis occurs with only two false alarms and sensitivity losses for a liquid-line restriction.

ACKNOWLEDGEMENTS

This work was supported by the California Energy Commission (CEC) with additional cost-sharing provided by Honeywell, Inc and Field Diagnostic Services, Inc.

NOMENCLATURE

α	= False alarm threshold
compleak	= Compressor valve leakage
condfoul	= Condenser fouling
COP	= Coefficient of performance
$\Delta^2 P_{ll}$	= Liquid-line filter/drier pressure difference residual
ΔT_{dis}	= Discharge line temperature residual
ΔT_{sc-sh}	= Refrigerant charge diagnosis feature
$\Delta \dot{V}_{ca}$	= Condenser air volume flow residual
$\Delta \dot{V}_{ea}$	= Evaporator air volume flow residual
EER	= Equipment efficiency ratio
evapfoul	= Evaporator fouling
FDD	= Fault detection and diagnosis
$fv_{current}$	= Current feature value
fv_{range}	= Feature value at an individual fault level causing approximately a 20% cooling capacity degradation
FXO	= Fixed orifice
$IND_{faultname}$	= Decoupling fault feature for a given fault
$IND_{i,MSF}$	= Fault indicator of fault i occurring simultaneously with other faults
$IND_{i,SF}$	= Fault indictor of fault i occurring individually,
$IND_{i,threshold}$	= FDD threshold of fault i
llrestr	= Liquid-line restriction
P_{dis}	= Discharge pressure
P_{down}	= Orifice outlet pressure
P_{ll}	= Liquid-line pressure
P_{suc}	= Suction pressure
P_x	= Expansion device upstream refrigerant temperature
ϕ_{oie}	= Evaporator inlet air relative humidity
$\dot{Q}_{cap}$	= Cooling capacity
refleak	= Refrigerant leakage

refover	=	Refrigerant overcharge
reflow	=	Refrigerant low charge
refunder	=	Refrigerant undercharge
ρ_i	=	Normalized indicator error for fault i
RTU	=	Rooftop unit
SHR	=	Sensible heat ratio
T_{aic}	=	Condenser inlet air temperature
T_{aie}	=	Evaporator inlet air temperature
T_{amb}	=	Compressor ambient air temperature
T_{aoc}	=	Condenser outlet air temperature
T_{aoe}	=	Evaporator outlet air temperature
T_{cond}	=	Condensing temperature
T_{dis}	=	Discharge line temperature
T_{down}	=	Expansion device downstream temperature
T_{evap}	=	Evaporating temperature
T_{sc}	=	Subcooling
T_{sh}	=	Superheat
TXV	=	Thermostatic expansion device

REFERENCES

[1] Li, H. and Braun, J. E., Evaluation of a Decoupling-Based Fault Detection and Diagnostic Technique – Part II: Field Evaluation and Application, The sixth International Conference for Enhanced Building Operations, Shenzhen, China, 2006. (accepted)

[2] Comstock, M.C., J.E. Braun, and Chen, B., Literature Review for Application of Fault Detection and Diagnostic Methods to Vapor Compression Cooling

[7] Li, H. and Braun, J. E., A Methodology for Diagnosing

Equipment, Purdue University, Ray W. Herrick Laboratories, 1999, Report # HL99-19.

[3] Li, H., A Decoupling-Based Unified Fault Detection and Diagnosis Approach for Packaged Air Conditioners, Ph.D. Thesis, School of Mechanical Engineering, Purdue University, 2004.

[4] Dexter, Arthur; Pakanen, Jouko et al., Demonstrating Automated Fault Detection and Diagnosis Methods in Real Buildings. Espoo. VTT Building Technology, 2001, VTT Symposium 217. 381 p. + app. 13 p.

[5] Katipamula, S. and Brambley, M., Methods for Fault Detection, Diagnostics, and Prognostics for Building Systems—A Review, Part I, International Journal of HVAC&R Research, 2005, vol. 11, No. 1, Page 3-25.

[6] Katipamula, S. and Brambley, M., Methods for Fault Detection, Diagnostics, and Prognostics for Building Systems—A Review, Part II, International Journal of HVAC&R Research, 2005,vol. 11, No. 2, Page 169-188.

Multiple-Simultaneous Faults in Vapor Compression Air Conditioners, International Journal of Heating, Ventilating, and Air Conditioning and Refrigerating Research, 2006. (accepted)

[8] Breuker, and Braun, J.E., Common Faults and Their Impacts for Rooftop Air Conditioners, HVAC&R Research, 1998,Vol. 4, No. 3, pp.303-318.

[9] Li, H. and Braun, J.E., "An Improved Method for Fault Detection and Diagnosis Applied to Packaged Air Conditioners". ASHRAE Transactions, 2003, Vol.109, Part 2.

[10] Li, H., and Braun, J. E., Decoupling Features and Virtual Sensors for Diagnosis of Faults in Vapor Compression Air Conditioners, International Journal of Refrigeration, 2006b. (accepted)